Article

A Closed Form Selected Mapping Algorithm for PAPR Reduction in OFDM Multicarrier Transmission †

Sara Carcangiu ![ORCID], Alessandra Fanni *![ORCID] and Augusto Montisci ![ORCID]

Department of Electrical and Electronic Engineering, University of Cagliari, Piazza D'Armi,
09123 Cagliari, Italy; sara.carcangiu@unica.it (S.C.); augusto.montisci@unica.it (A.M.)
* Correspondence: fanni@unica.it; Tel.: +39-070-675-5870
† This paper is an extended version of our paper published in 2016 Civil-Comp Proceedings volume 110,
pp. 1–17.

Abstract: Nowadays, the demand for communication multi-carriers' channels, where the sub-channels are made mutually independent by using orthogonal frequency division multiplexing (OFDM), is widespread both for wireless and wired communication systems. Even if OFDM is a spectrally efficient modulation scheme, due to the allowed number of subcarriers, high data rate, and good coverage, the transmitted signal can present high peak values in the time domain, due to inverse fast Fourier transform operations. This gives rise to high peak-to-average power ratio (PAPR) with respect to single carrier systems. These peaks can saturate the transmitting amplifiers, modifying the shape of the OFDM symbol and affecting its information content, and they give rise to electromagnetic compatibility issues for the surrounding electric devices. In this paper, a closed form PAPR reduction algorithm is proposed, which belongs to selected mapping (SLM) methods. These methods consist in shifting the phases of the components to minimize the amplitude of the peaks. The determination of the optimal set of phase shifts is a very complex problem; therefore, the SLM approaches proposed in literature all resort to iterative algorithms. Moreover, as this cal-culation must be performed online, both the computational cost and the effect on the bit rate (BR) cannot be established a priori. The proposed analytic algorithm finds the optimal phase shifts of an approximated formulation of the PAPR. Simulation results outperform unprocessed conventional OFDM transmission by several dBs. Moreover, the complementary cumulative distribution function (CCDF) shows that, in most of the packets, the proposed algorithm reduces the PAPR if compared with randomly selected phase shifts. For example, with a number of shifted phases $U = 8$, the CCFD curves corresponding to the analytical and random methods intersect at a probability value equal to 10^{-2}, which means that in 99% of cases the former method reduces the PAPR more than the latter one. This is also confirmed by the value of the gain, which, at the same number of shifted phases and at the probability value equal to 10^{-1}, changes from 2.09 dB for the analytical to 1.68 dB for the random SLM.

Keywords: power lines communication; peak-to-average-power ratio; selected mapping; analytical solution

1. Introduction

Orthogonal frequency division multiplexing (OFDM) is an efficient multi-carrier modu-lation technique both for wireless communication and power line communication (PLC).

For its high data rate, OFDM has been indeed widely used in many wireless commu-nication standards, such as digital video broadcasting (DVB) and based mobile worldwide interoperability for microwave access [1]. It offers a considerable high spectral efficiency, multipath delay spread tolerance, immunity to the frequency selective fading channels and power efficiency [2,3].

Moreover, the rapid development of smart grids and electric transportation has made PLC technology a promising complementary scheme to the wireless communications [4–8].

In such a case, OFDM has been proposed to overcome the limited bandwidth (up to 100 MHz) and enhance the transmission throughput in PLC systems; the power line is exploited as a communication multi-carriers' channel, where the sub-channels are made mutually independent by using orthogonal frequencies. In 2010, the standard IEEE 1901 has been approved to unify PLC technologies based on OFDM modulation scheme for high-speed communication devices using frequencies below 100 MHz [9].

Despite the great advantages that OFDM modulation scheme presents in both wireless and power line communications, some important aspects need to be addressed in the systems design. One of the major issues is the high peak-to-average power ratio (PAPR) of the transmitted OFDM signals, which depends on the phases of the sub carriers.

These peaks could decrease the signal-noise ratio (SNR) of the digital-to-analog converter (DAC). Moreover, they could saturate the transmitting high-power amplifiers (HPA), overcoming their dynamic range and modifying the shape of the OFDM symbol, and then affecting its information content. Furthermore, such spikes bring problems of electromagnetic compatibility that, in many applications, put very strict requirements, due to the presence of critical electrical devices.

Many approaches have been proposed to deal with the PAPR reduction problem, and literature reports several review papers that propose different classifications of the methods [10–13]. They mainly categorized the methods in the following classes:

1. Coding techniques (CT), which avoid the use of codeword with high peak power [14–20];
2. Signal distortion techniques (SD), such as clipping and filtering, which means the non-linear treatment of amplitude near the peak power [21–23];
3. Multiple signaling and probabilistic techniques (MSP), such as selected mapping methods (SLM) [24–26], partial transmission sequence (PTS) [27,28], phase optimization [29], tone reservation and tone injection [30], and constellation shaping [31,32], which generate a permutation of the multi-carrier signal and choose the signal with the minimum PAPR for transmission, or modify different parameters in the OFDM signal, and optimize them to minimize the PAPR.

Over the last few years, several studies have been presented, which combine two or more PAPR reduction methods to use the characteristics of each method in a hybrid scheme to improve performance and to improve the cost efficiency in terms of better PAPR reduction [33]. Among these techniques, in literature there are some that combine the approach of selective mapping (SLM) with other approaches, often demonstrating advantages in terms of complexity and/or information integrity. In [34] two parallel forms of multiple signal representation (MSR) approaches, the SLM methodology and the modified-partial transmit sequence (PTS) technique called the cyclic shift sequences, PTS are mixed to enhance the PAPR efficiency and computational complexity level better than the conventional PTS methodology. In [35,36], SLM methods are used with compounding methods. The latter are applied to speech signal having high peaks and are also applied to the OFDM signal. In particular in [36], a new hybrid method has been proposed considering the cascade of two stages. In the first stage, the SLM is combined with PTS reduction technique and in the second stage the PTS technique is combined with compounding methods. This hybrid method is able to reduce the system complexity and to increase the bit error rate performance. In order to reduce the complexity of SLM and achieve a significant PAPR reduction, in [37] the authors propose a hybrid approach called low complexity hybrid selective mapping for PAPR mitigation for asymmetrically clipped optical OFDM. The new approach utilizes the properties of IFFT and Hermitian symmetry to reduce the complexity of the conventional SLM. Despite the great number of methods, until now, no one has been able to solve the problem at low computational cost and, at the same time, preserving the information content of the signal.

In [38], a detailed analysis of advantages/limitations of several approaches that combine SLM and PTS is reported. This analysis shows that there is a trade-off between the efficiency in the PAPR reduction and the computational complexity level of these hybrid methods.

Our proposal focuses on improving the performance of the SLM method, which is one of the most used in hybrid approaches. The SLM [25] approach consists in applying a phase shift to the components of the OFDM symbol, changing the shape of the OFDM symbol in such a way to limit the peaks. The determination of the optimal set of phase shifts is a very complex problem; thus, the SLM approaches proposed in literature all resort to iterative algorithms to solve it. In this paper, the problem of determining the optimal set of phase shift is solved in closed form on an approximated formulation of the PAPR. Such approximation uses the n-norm instead of infinity norm, with $n = 4$, in the definition of the PAPR. The gradient expression of the objective function has been analytically defined, and its solution consists simply in the calculation of the roots of a sixth degree polynomial, which represent the optimal solutions of the optimization problem. To better approximate the PAPR value, the analytical evaluation can be easily extended to a greater value of the n-norm. We have limited ourselves to $n = 4$ in order not to burden the reading of the analytical steps of the algorithm reported in the Appendix A of the paper. However, the proposed approach can be conceptually extended to a higher value of n at the expense of a higher number of analytical steps. Simulation results demonstrate the validity of the n-norm approximation and the advantage with respect to SLM iterative methods.

The paper is organized as follows. Section 2 introduces the OFDM system model. In Section 3, the PAPR problem is depicted together with the selected mapping method. In Section 4, the closed form algorithm is proposed, whereas the simulation results are reported in Section 5. The last Section 6 provides discussion and conclusions. Finally, in the Appendix A, the analytical steps are reported.

2. OFDM System Model

Figure 1 shows the basic scheme of an OFDM system. An OFDM modulation scheme allows digital data to be efficiently and reliably transmitted over a transmitter channel and it performs well even in multipath environments with reduced receiver complexity. Using ODFM, it is possible to exploit the time domain, the space domain, the frequency domain and even the code domain to optimize transmitter channel usage. As shown in Figure 1, the bit data must be firstly converted from serial stream into parallel streams, each of which are coded and modulated on to a subcarrier. In fact, OFDM allows one to subdivide the available band into mutually orthogonal subcarriers so that each of them can be considered independently. These subcarriers are regularly spaced in frequency, forming a block of spectrum. The frequency spacing and time synchronization of the subcarrier is chosen in such a way that the subcarriers are orthogonal, which means they do not cause interference with one another. Moreover, using narrow subcarriers, the frequency response can be considered constant and then the signal does not undergo distortion effects.
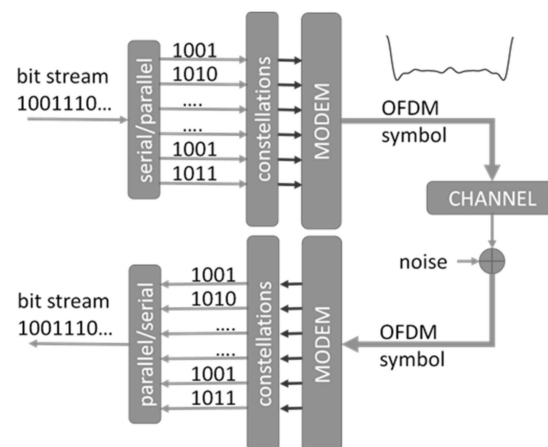

Figure 1. Basic schema of an OFDM transmitter and receiver (T/R) system.

The signal sent through the single sub channel is the sum of two iso frequential in quadrature sinusoidal signals. The two degrees of freedom, given by the amplitude of the two sinusoids, allow one to send a two-dimensional message, corresponding to points in the plane (Figure 2). The set of points constitutes a constellation, and each point is associated with a binary string; therefore, the more points, the more bits are associated to each point, and then the higher the bit rate. In Figure 2, two different kinds of constellation are shown: the amplitude phase shift keying (APSK), and the quadratic amplitude modulation (QAM).
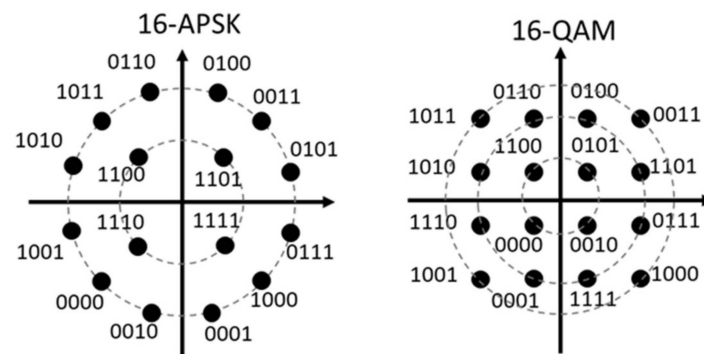

Figure 2. APSK and QAM modulation schemes.

Each constellation is associated with a maximum power level, corresponding to the farthest points from the origin. To increase the number of points and then the length of the string associated to each of them, one can augment the power available for the sub channel or put the points closer each other. Note that, the first solution can give rise to saturation of the transmission devices and interferences, whereas the second solution can cause receiving errors, due to the unavoidable presence of noise. The QAM scheme is more diffused than the APSK because it is easier to implement, and the average signal power is lower. However, in this work, to cope with possible heavy noise conditions, we preferred to adopt the APSK constellation scheme.

3. PAPR in OFDM Systems

The OFDM typically suffers a high peak to average power ratio (PAPR), defined for transmitted signal $x(t)$, as

$$\text{PAPR}[x(t)] = \frac{peak\ power\ of\ x(t)}{average\ power\ of\ x(t)} = \frac{\max\limits_{0 \le t \le T} |x(t)|^2}{\frac{1}{T} \int_0^T |x(t)|^2 dt} \tag{1}$$

where T is the interval of OFDM signal (OFDM symbol period).

PAPR has negative consequences, both on the interference caused, for example, by PLC transmission and on the allowed peak of power the system can support. In particular, if the instantaneous signal overcomes the linear range of the amplifier, this clips the peaks of the signal, which will result in distorted [39].

Selected Mapping Approach for PAPR Reduction

Selected mapping approach basically consists of shifting the phase of the sinusoidal components in order to reduce the value of the peaks. As previously highlighted, although SLM is one of the most used PAPR reduction techniques, it has some drawbacks. In fact, typically this approach is applied online, because a different set of phase shifts must be determined for any stream of bit and it is not reasonable calculating a priori the shifting for all the possible streams, but this implies that the set of phases before the shifting has to be sent as side information, by using to this purpose a part of the available channel. Note that, the reduction of the PAPR, whichever approach is used, is paid in terms of bit rate.

Most of the SLM approaches presented in literature consist in iteratively generating a large set of phase shift vectors, and then selecting the OFDM symbol having the lowest PAPR. The quality of the solution in terms of low PAPR depends on the number of phase shift vectors. However, the required calculation time must not exceed the rate the streams are generated, so as not to affect the transmission rate.

In [40], it is shown that the iterative procedure usually converges towards a limited set of phases to shift, because the incremental benefit that can be obtained by shifting the most parts of the components is very low.

This fact suggests that a possible way to reduce the computational cost is to select a reduced number of phases to shift. Limiting the number of phases to shift has a benefit in terms of bit rate, because it reduces the side information of the transmission. Indeed, if the point of the constellation undergoes a phase shifting, this shift must be attached to the transmission, to make it possible for the receiver to reconstruct the original message. Therefore, the higher the number of shifted components, the higher is the part of the channel used to transmit side information.

In this work, the number of phases to be shifted is established a priori. The components whose phase is shifted are those having the highest values of power, which are potentially those mainly affecting the PAPR. In this way, the receiver can deduce the set of shifted components without any side information. To overcome the computational complexity of the algorithm, in this paper, the problem of finding the optimal phase shift vector is solved in closed form on an approximated formulation of the PAPR.

To compare the results of a PAPR reduction technique it is common to refer to the complementary cumulative distribution function (CCDF) of the PAPR, which provides a statistical description of the power levels in the OFDM signal. In particular, it gives the probability that PAPR of the OFDM signal $x(t)$ will be above a given threshold $PAPR_0$ [10].

A PAPR reduction algorithm may satisfy the multiple objectives of reducing the PAPR without affecting the bit rate (BR) and the bit error rate (BER), hence limiting the computational complexity and the side information to be transmitted. Several performance indexes can be introduced. As SLM algorithms do not affect BER, in this paper the following performance index has been proposed [13]:

$$\Gamma = -10log_{10}\left(\frac{PAPR_{after}}{PAPR_{before}}\right) \tag{2}$$

which measures the relative PAPR reduction after the application of the algorithm at a fixed CCDF. A large value for the "gain" Γ implies better PAPR reduction.

4. Analytical Solution of SLM Problem

The calculation of the optimal phase shift vector is a hard task, which could require a high computational cost even in the case of a small number of phases to shift. The complex envelope of the transmitted OFDM signal can be written as:

$$x(t) = \frac{1}{M}\sum_{k=-M}^{M} X_k e^{jk\omega t}, \ 0 \le t \le MT \tag{3}$$

where $X = \{X_k, \ k = -M, \cdots, M\}$ is the block of M symbols, M is the number of subcarriers, ω is the angular frequency of the fundamental harmonic, and $j = \sqrt{-1}$.

The equivalent real envelope can be obtained by summing M sinusoids corresponding to as many subcarriers:

$$x(t) = \sum_{k=1}^{M} A_k \sin(k\omega t + \varphi_k) \tag{4}$$

The aim of the optimization problem consists in minimizing the PAPR value given by (1) of the OFDM symbol (4) acting on a prefixed number U of phases φ_k. The initial values of both amplitudes A_k and phases φ_k depend on the current frame of bits transmitted

with the OFDM symbol, so that a new optimization problem must be solved online for each symbol.

The first objective is to remove the time variable in the formulation of the optimization problem. In fact, it is a difficult task to foresee the position of the peaks in the OFDM symbol, and this would be a further problem to address inside that of optimizing the PAPR. To this end, we resort to the norm of the signal, which is defined for the generic order n as:

$$E^n = \sqrt[n]{\int_0^T |x(t)|^n dt} \tag{5}$$

As it is well known, as $n \to \infty$, E^n tends to the maximum value of $x(t)$, but, in general, a small order $n > 2$ is sufficient to put in evidence the presence of an instantaneous peak. In particular, we can observe that the integral inside the root in (5), for $n = 2$ is equal to the energy of $x(t)$, which is invariant with respect to the phases φ_k of its components.

Therefore, even for $n = 3$, the norm could be used to estimate the presence of a peak in the signal. For the sake of simplicity, the norm $n = 4$ has been adopted, to avoid introducing the absolute value of the objective function. Furthermore, the root operation in (5) does not affect the position of the minimum, so that the optimization problem is formalized as follows:

$$\min_{\varphi \in \Phi} \left\{ P = \int_0^T x(t)^4 dt \right\} \tag{6}$$

where Φ is the set of phases to shift and P is a function whose stationary points are assumed in place of those of the PAPR$[x(t)]$. Figure 3 reports PAPR$[x(t)]$ (continuous red line) and P (continuous blue line) when changing only one phase angle from $0°$ to $360°$. As expected, the two curves present an offset, due to their different definitions, but their minimums (highlighted with vertical dashed lines) are quite close and, assuming the stationary point evaluated on the blue curves, non-significant variation is introduced in the PAPR. Note that, a further improvement of the PAPR approximation can be achieved if a norm n, with n greater than 4, is considered, at the cost of a greater effort in the analytic determination of the optimal phase shifts. In the same Figure 3, the continuous green line reports the trend of P evaluated using the norm $n = 16$ instead of $n = 4$. As can be noted, the offset greatly reduces and the two minima points almost coincide.
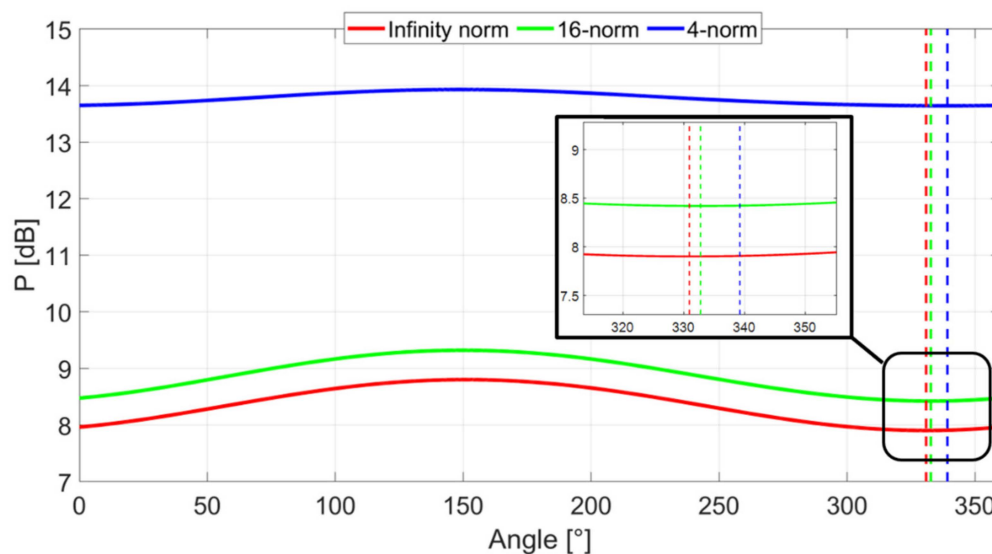

Figure 3. Continuous lines: Approximated PAPR P with norm $n = 4$ (blue), norm $n = 16$ (green) and norm $n = \infty$ (red) when changing only one phase angle from $0°$ to $360°$. Vertical dashed lines show (with the same color) the minimum of the three curves. A zoom of the minimum points is reported in the frame.

Considering (4) and (6), the general expression of the norm P can be calculated, where the fundamental frequency ω has been normalized to 1:

$$P = \int_0^{2\pi} \left[\sum_{k=1}^M A_k \sin(kt + \varphi_k) \right]^4 dt \tag{7}$$

In this paper, a line search algorithm [41] is used to seek the minimum of the objective function. To this end, the gradient expression of the objective function must be defined, in order to calculate the stationary points. It is worth noticing that this does not affect the generality of the results. By deriving (7) with respect to $\varphi_r \in \Phi$, the first-order condition can be determined:

$$\frac{\partial P}{\partial \varphi_r} = 4 \int_0^{2\pi} \left[\sum_{k=1}^M A_k \sin(kt + \varphi_k) \right]^3 A_r \cos(rt + \varphi_r) \cdot dt = 0 \tag{8}$$

Let us re-write Equation (8) highlighting the r-th term in the sum:

$$\frac{\partial P}{\partial \varphi_r} = 4 \int_0^{2\pi} \left[A_r \sin(rt + \varphi_r) + \sum_{\substack{k=1 \\ k \neq r}}^M A_k \sin(kt + \varphi_k) \right]^3 \cdot A_r \cos(rt + \varphi_r) dt = 0 \tag{9}$$

Let us define $s_k = \sin(kt + \varphi_k)$ and $c_k = \cos(kt + \varphi_k)$. Then, the first order condition becomes:

$$\frac{\partial P}{\partial \varphi_r} = \int_0^{2\pi} \left(A_r s_r + \sum_{\substack{k=1 \\ k \neq r}}^M A_k s_k \right)^3 \cdot A_r c_r \, dt =$$

$$= \int_0^{2\pi} \left[A_r^3 s_r^3 + 3 A_r^2 s_r^2 \sum_{\substack{k=1 \\ k \neq r}}^M A_k s_k + 3 A_r s_r \left(\sum_{\substack{k=1 \\ k \neq r}}^M A_k s_k \right)^2 \right.$$

$$\left. + \left(\sum_{\substack{k=1 \\ k \neq r}}^M A_k s_k \right)^3 \right] \cdot A_r c_r \, dt = 0 \tag{10}$$

The four terms in Equation (10) can be evaluated separately in closed form by simple analytical steps, reported in Appendix A, leading to:

First Term

$$\int_0^{2\pi} A_r^3 s_r^3 A_r c_r \, dt = 0, \, \forall r \tag{11}$$

Second Term

$$\int_0^{2\pi} \left(3 A_r^2 s_r^2 \sum_{\substack{k=1 \\ k \neq r}}^M A_k s_k \right) A_r c_r \, dt = A \cos(3\varphi_r) + B \sin(3\varphi_r) \tag{12}$$

where

$$\begin{cases} A = -\frac{3}{8} 2\pi A_r^3 A_k \sin(\varphi_k) \\ B = \frac{3}{8} 2\pi A_r^3 A_k \cos(\varphi_k) \end{cases} \tag{13}$$

Third Term

$$\int_0^{2\pi} 3A_r s_r \left(\sum_{\substack{k=1 \\ k \neq r}}^{M} A_k s_k \right)^2 A_r c_r \, dt = C cos(2\varphi_r) + D sin(2\varphi_r) \tag{14}$$

where

$$\begin{cases} C = \pm \frac{3}{4} 2\pi A_r^2 \sum_{\substack{k \pm m = 2r \\ k, m \neq r \\ k > m}}^{M} A_k A_m \sin(\varphi_k \pm \varphi_m) \\ D = \mp \frac{3}{4} 2\pi A_r^2 \sum_{\substack{k \pm m = 2r \\ k, m \neq r \\ k > m}}^{M} A_k A_m \cos(\varphi_k \pm \varphi_m) \end{cases} \tag{15}$$

Fourth Term

$$\int_0^{2\pi} \left(\sum_{\substack{k=1 \\ k \neq r}}^{M} A_k s_k \right)^3 A_r c_r \, dt = E \cos(\varphi_r) + F \sin(\varphi_r) \tag{16}$$

where

$$\begin{cases} E = \pm \frac{3}{4} 2\pi A_r \sum_{\substack{k+l \mp m \\ k,l,m \neq r \\ k > l > m}}^{M} A_k A_l A_m \sin[\varphi_k \pm (\varphi_l \mp \varphi_m)] \\ F = \mp \frac{3}{4} 2\pi A_r \sum_{\substack{k+l \mp m \\ k,l,m \neq r \\ k > l > m}}^{M} A_k A_l A_m \cos[\varphi_k \pm (\varphi_l \mp \varphi_m)] \end{cases} \tag{17}$$

Determination of φ_r

In the following, the phases φ_r, corresponding to the stationary points, are deduced.

Once the coefficients, A, B, C, D, E and F, whose derivation is reported in the Appendix A, are evaluated in closed form, the first-order condition (10) becomes:

$$\frac{\partial P}{\partial \varphi_r} = A \cos(3\varphi_r) + B \sin(3\varphi_r) + C \cos(2\varphi_r) + D \sin(2\varphi_r) + E \cos(\varphi_r)$$
$$+ F \sin(\varphi_r) = 0 \tag{18}$$

Applying the Weierstrass substitution (or tangent half-angle substitution) [42], which introduces the variable $z = tan\left(\frac{\varphi_r}{2}\right)$, the following parametric trigonometric relations can be stated:

$$sin(\varphi_r) = \frac{2z}{1+z^2} \quad ; \quad cos(\varphi_r) = \frac{1-z^2}{1+z^2} \tag{19}$$

Then, using the duplication and triplication formulas, it follows that:

$$\sin(2\varphi_r) = 2sin(\varphi_r)cos(\varphi_r) = \frac{4(z - z^3)}{(1 + z^2)^2} \tag{20}$$

$$cos(2\varphi_r) = cos^2(\varphi_r) - sin^2(\varphi_r) = \frac{z^4 - 6z^2 + 1}{(1 + z^2)^2} \tag{21}$$

$$sin(3\varphi_r) = 3sin(\varphi_r) - 4sin^3(\varphi_r) = \frac{6z^5 - 20z^3 + 6z}{(1 + z^2)^3} \tag{22}$$

$$cos(3\varphi_r) = 4\cos^3(\varphi_r) - 3cos(\varphi_r) = \frac{-z^6 + 15z^4 - 15z^2 + 1}{(1 + z^2)^3} \tag{23}$$

Hence, the first-order condition becomes:

$$\begin{aligned}
\frac{\partial P}{\partial \varphi_r} = &(-A + C - E)\, z^6 + (6B - 4D + 2F)\, z^5 + (15A - 5C - E)\, z^4 \\
&+ (-20B + 4F)\, z^3 + (-15A - 5C + E)\, z^2 \\
&+ (6B + 4D + 2F)\, z + (A + C + E) = 0
\end{aligned} \tag{24}$$

Solving this equation with respect to z, the values of φ_r are obtained as:

$$\varphi_r = 2\tan^{-1}(z) \tag{25}$$

It is worth to point out that the phase φ_r, corresponding to the stationary point, is not unique, because it is obtained as the argument of a trigonometric function. This is in accordance with the fact that the stationary point could be either a minimum or a maximum point.

5. Simulation Results

Following the analytical procedure described in previous Sections, a first simulation has been conducted by considering a random bit stream composed of 10^7 bits and OFDM symbols with 64-APSK modulation to present the statistical analysis of the PAPR reduction by varying the number of shifted phases U. In the simulation, an OFDM base-band signal with $N = 64$ subcarriers and 390,625 frames has been considered.

In Figure 4, the comparison between the PAPR CCDF curves, obtained with the conventional OFDM and the SLM method with a number U of shifted phases ranging from 2 to 32, is reported. It can be observed that a small number of shift vectors allows the PAPR to be strongly reduced, but at the same time at the improvement tends to saturate very soon.

Figure 5 reports the marginal improvement of the gain Γ of the random SLM method with the increase of the number U of shifts from 2 to 32. The gain has been calculated for CCDF equal to 10^{-3}. As can be noted, the PAPR reduction tends to saturate as the number of shift vectors increases, and no further measurable advantage can be achieved with a number of shift vectors greater than eight.

The proposed analytic SLM has been tested on the same bit stream used for the above analysis. In Figure 6, the CCDF diagrams are shown for different numbers of shifted carriers for the analytical SLM and the random SLM. As can be observed, for $U = 8$, the analytical SLM outperforms the random one in the overwhelming majority of the cases, while the latter works better in the rare cases where the PAPR is very high.
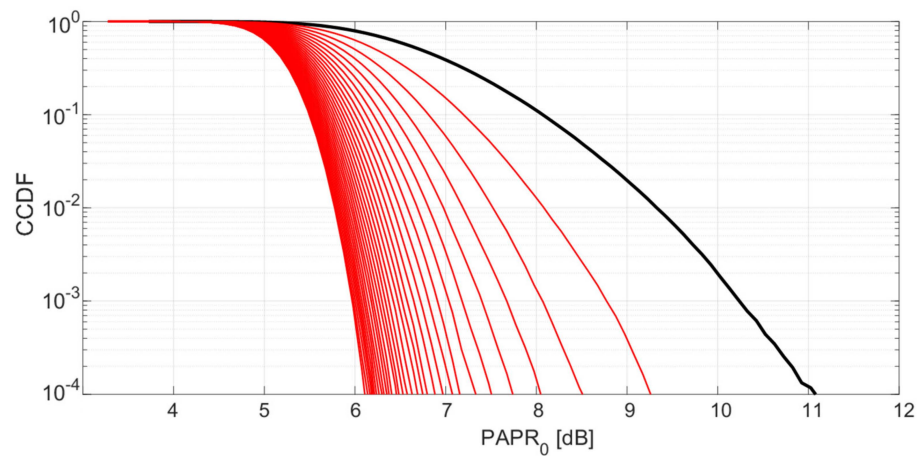
Figure 4. Comparisons of CCDF in OFDM-APSK system for conventional OFDM (black) and for the random SLM PAPR reduction technique with *U* ranging from 2 to 32, step 1 (red, from right to left).
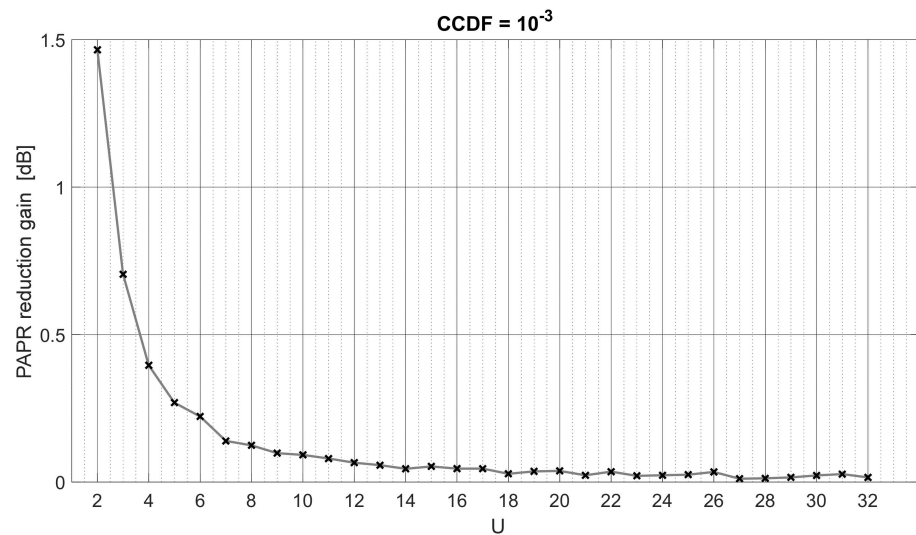

Figure 5. Marginal improvement of PAPR reduction gain of the random SLM method with the increase of number *U* with CCDF = 10^{-3}.
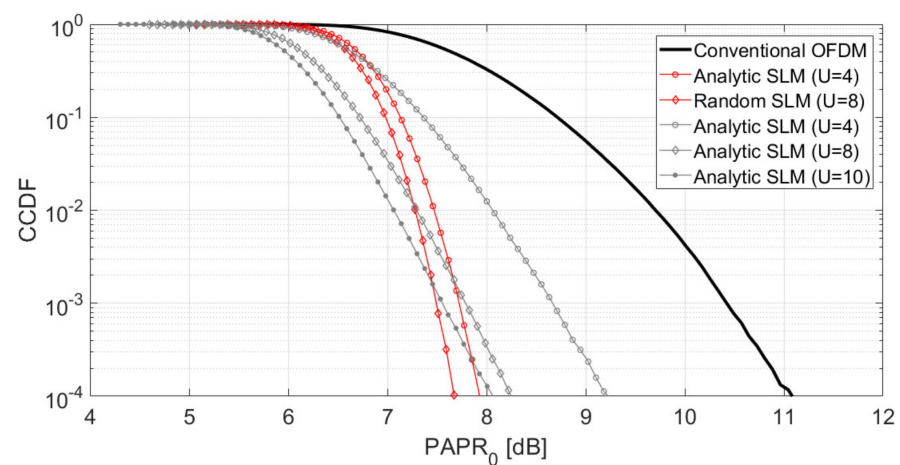

Figure 6. Comparisons of CCDF in OFDM-APSK system for conventional OFDM (bold black), random (red), and analytic (grey) PAPR reduction techniques with *U* = 4 (circle), *U* = 8 (diamond), and *U* = 10 (stars).

This is confirmed by the values reported in Table 1, which presents the comparison between the analytic and the random SLM in terms of the gain Γ. Three cases are reported corresponding to three different values of CCDF. The larger values of Γ for analytic SLM for higher values of CCDF implies its better PAPR reduction in the large majority of cases. However, as already highlighted, with the random SLM algorithm, the maximum value of the PAPR reduction can be obtained with a limited number of phase shift vectors and, due to the low computational cost, it would be possible to apply in parallel the two algorithms and, for each frame, the one corresponding to the maximum reduction can be assumed to calculate the OFDM symbol. In this case, the effective CCDF curve is represented by the leftmost envelope of the random and analytical diagrams.

Table 1. Gain of PAPR reduction techniques with $N = 64$ and $U = 8$.

PAPR Reduction Technique	CCDF= 10^{-3}	CCDF= 10^{-2}	CCDF= 10^{-1}
Analytical approach	2.89	2.43	2.09
Random SLM	2.94	2.43	1.68
DSLM [43]	2.97	2.63	1.93

Although the example referred to in Figure 6 is very basic, the results allow some important considerations to be made. The first is that the improvements achieved with the random approach tend to saturate for low values of U. In the real cases, in which the number of subcarriers is much higher than in the example, the saturation phenomenon will be even more evident, because the relative weight of the proposed random solutions will be much smaller. Another aspect that appears evident is that, with the same number of shifted phases, the proposed method allows one to obtain a greater reduction in PAPR in most cases. For example, with $U = 8$, the curves corresponding to the random and analytical methods intersect at a probability value equal to 10^{-2}; this means that in 99% of cases the analytical method reduces the PAPR more. In 1% of cases, the random method allows for a better result. This fact is attributable to the fact that a low-order norm was adopted. As shown in Figure 3, as the order of the norm increases, the minimum point of the norm tends to coincide with the global minimum, so that the growth of the norm necessarily involves a shift to the left of the curve in Figure 6. As explained previously, the adoption of a higher order norm does not involve a greater computational burden during transmission, but only a greater analytical development of the model.

For the sake of comparison, in the same Table 1, the values of the gain provided in recent literature [43], by using the dispersive selection mapping (DSLM) scheme proposed in [44], have been added for the same number N of subcarriers and the same number U of phases shifted. Even if the DSLM presents limited advantages with respect to analytic and random SLM at a probability value equal to 10^{-2}, the analytic SLM outperforms both random and DSLM at a probability value equal to 10^{-1}. Note that DSLM has a higher computational complexity with respect to analytic and random SLM.

6. Discussion and Conclusions

The OFDM is a very appealing technique both for wireless and wired communications because of its spectrum efficiency and robust channel. One of its main disadvantages is that the composite transmitted signal may present a very high peak to average power ratio (PAPR) when the input sequences are strongly correlated. Hence, PAPR reduction is mandatory. A PAPR reduction algorithm may satisfy the multiple objectives of reducing the PAPR without affecting the bit rate (BR) and the bit error rate (BER), hence limiting the computational complexity and the side information to be transmitted.

In this paper, a closed form algorithm for the PAPR reduction in OFDM modulation scheme is proposed, which can be used both in wired and wireless communications. It represents an analytical solution of the optimization problem associated with the selective

mapping (SLM) method, where the peaks occurring in the multi carrier signals are reduced by applying a phase shifting to the sinusoidal components of the signal. The analytical solution is obtained by an approximation of the PAPR definition, which uses the *n-norm* instead of *infinity-norm*, with *n* = 4, in the definition of the PAPR, and it presents several advantages with respect to the random SLM iterative approaches presented in literature.

Firstly, the analytically obtained solution represents the optimal solution of the minimization problem if the approximation introduced by replacing *4-norm* with the *infinity-norm* in the definition of the PAPR is disregarded. Note that, the closed-form algorithm can be formulated using *n-norm* with increased value of *n*, achieving a better approximation of PAPR at the cost of increased effort in off-line analytical steps. In this paper, the order *n* = 4 has been adopted just so as not to burden the analytical steps reported in the Appendix A.

Moreover, the computational time of the random SLM method to define the phase shift is not fixed. In fact, a certain number of random attempts are performed, until the value of the PAPR is acceptable or no improvement is obtained after a prefixed maximum number of runs. Conversely, the computational complexity of the proposed closed form method is limited to the solution of a 6th degree polynomial equation, which guarantees that the best solution is found in a fixed time.

The potentiality of the proposed approach has been tested referring to a case study and comparison has been made with the random SLM PAPR reduction gain with respect to the conventional OFDM.

As shown in the results, with the same number of candidate phase vectors U with $U > 4$, the random SLM method exceeds the analytical SLM in the rare cases where the PAPR is very high, while the former works better in the vast majority of cases. Even with a number of shifted phases $U = 8$, the CCFD curves corresponding to the analytical and random methods intersect at a probability value equal to 10^{-2}. This means that in 99% of cases the first method reduces the PAPR more than the second one. This is also confirmed by the value of the gain Γ, which measures the relative PAPR reduction after the application of the algorithm at a fixed CCDF. The larger the value of the gain, the better the PAPR reduction. With a number of shifted phases $U = 8$ and at the probability value equal to 10^{-2} the gain assumes the same value $\Gamma = 2.43$ dB for both the analytic and random methods, whereas at the probability value equal to 10^{-1}, $\Gamma = 2.09$ dB for the analytical and $\Gamma = 1.93$ dB for the random SLM. From the comparison with literature [43], analogue conclusions can be drawn.

The results could be improved if a better approximation of the PAPR is considered by increasing the norm order, at the cost of further offline effort in the analytic determination of the stationary points.

Note that, while with random SLM the computational complexity increases with the increase of U, and, at the same time, the relative improvement decreases, with the analytical approach, the computational complexity does not change with the increase of U while maintaining significant margins for improvement.

Recently, several hybrid approaches have been proposed to minimize the PAPR value, at the expense of increasing the computational complexity. Literature clearly demonstrates that the most promising approach is to combine two or more PAPR reduction methods to use the characteristics of each method in a hybrid scheme. However, there is a trade-off between the efficiency in the PAPR reduction and the computational complexity level of these hybrid methods. Improving the performance of each of the methods in the hybrid approach will improve the efficiency of the overall hybrid method. Many of them combine the approach of selective mapping (SLM) with other approaches, such as the partial transmit sequence (PTS) methods [34,36]. Our proposal focuses on improving the performance of the SLM method, which is in fact one of the most used in hybrid approaches. The proposed closed form SLM algorithm, which per se is not superior to other methods, is not intended as an alternative to these recent hybrid methods, but, if ever, as an improvement of the SLM approach present in the hybrid methods with consequent impact on both the computational complexity of hybrid methods and the computational times.

A comparison with the most performing techniques will be done in future works by implementing the proposed analytical SLM approach within hybrid techniques. Moreover, in future works, the analytic approach will be extended to a higher value of norm order.

Data Availability Statement: No new data were created or analyzed in this study. Data sharing is not applicable to this article.

Appendix A

In this appendix, the four terms in Equation (10) are evaluated in closed form and the phases φ_r, corresponding to the stationary points, are deduced.

First Term

$$\int_0^{2\pi} A_r^3 s_r^3 A_r c_r \, dt = A_r^4 \int_0^{2\pi} s_r^3 c_r \, dt = A_r^4 \int_0^{2\pi} s_r^2 s_r c_r \, dt \tag{A1}$$

Applying the double-angle formulas to s_r^2 and the Werner formulas to $s_r c_r$:

$$A_r^4 \int_0^{2\pi} s_r^2 s_r c_r \, dt = \frac{A_r^4}{4} \int_0^{2\pi} (1 - c_{2r}) s_{2r} \, dt = \frac{A_r^4}{4} \int_0^{2\pi} \left(s_{2r} - \frac{1}{2} s_{4r} \right) dt = 0, \; \forall r \tag{A2}$$

The first term of (10) is null $\forall r$ because it is equal to the integral of two sinusoids within a multiple of their period.

Second Term

$$\int_0^{2\pi} \left(3 A_r^2 s_r^2 \sum_{\substack{k=1 \\ k \neq r}}^{M} A_k \; s_k \right) A_r c_r \, dt = 3 A_r^3 \sum_{\substack{k=1 \\ k \neq r}}^{M} A_k \int_0^{2\pi} s_k s_r^2 c_r \, dt$$

$$= \frac{3}{2} A_r^3 \sum_{\substack{k=1 \\ k \neq r}}^{M} A_k \int_0^{2\pi} s_k (1 - c_{2r}) c_r \, dt \tag{A3}$$

$$= \frac{3}{2} A_r^3 \sum_{\substack{k=1 \\ k \neq r}}^{M} A_k \int_0^{2\pi} (s_k c_r - s_k c_r c_{2r}) \, dt$$

The first term of (A3) leads to the sum of integrals whose argument is the product of two sinusoids with different frequency (because $k \neq r$); therefore, it is null $\forall r$. Concerning the second term, applying the Werner formulas to $c_{2r} c_r$, the following formula is obtained:

$$-\frac{3}{2} A_r^3 \sum_{\substack{k=1 \\ k \neq r}}^{M} A_k \int_0^{2\pi} s_k c_r c_{2r} \, dt = -\frac{3}{4} A_r^3 \sum_{\substack{k=1 \\ k \neq r}}^{M} A_k \int_0^{2\pi} (s_k c_r + s_k c_{3r}) \, dt \tag{A4}$$

The first addend in (A4) leads to the sum of integrals whose argument is the product of two sinusoids with different frequency (because $k \neq r$); therefore, it is null $\forall r$. For what concerns the second addend:

$$-\frac{3}{4}A_r^3 \sum_{\substack{k=1 \\ k \neq r}}^{M} A_k \int_0^{2\pi} s_k c_{3r} \, dt \neq 0 \ \forall \, k : k = 3r \tag{A5}$$

Then, the integral (A5) is not null for $k = 3r$. In fact, writing the expression (A5) in the extended form, and using the Werner formulas, and considering $k = 3r$:

$$-\frac{3}{4}A_r^3 \sum_{\substack{k=1 \\ k \neq r}}^{M} A_k \int_0^{2\pi} \sin(kt + \varphi_k)\cos(3rt + 3\varphi_r)dt$$

$$= -\frac{3}{8}A_r^3 \sum_{\substack{k=1 \\ k \neq r}}^{M} A_k \int_0^{2\pi} [\sin((k+3r)t + \varphi_k + 3\varphi_r)$$

$$+ \sin(\varphi_k - 3\varphi_r)]dt = -\frac{3}{8}2\pi A_r^3 \sum_{\substack{k=1 \\ k \neq r}}^{M} A_k \sin(\varphi_k - 3\varphi_r) \tag{A6}$$

$$= -\frac{3}{8}2\pi A_r^3 A_k \sin(\varphi_k - 3\varphi_r)$$

$$= -\frac{3}{8}2\pi A_r^3 A_k[\sin(\varphi_k)\cos(3\varphi_r) - \cos(\varphi_k)\sin(3\varphi_r)]$$

$$= \left[-\frac{3}{8}2\pi A_r^3 A_k \sin(\varphi_k)\right]\cos(3\varphi_r)$$

$$+ \left[\frac{3}{8}2\pi A_r^3 A_k \cos(\varphi_k)\right]\sin(3\varphi_r) = A\cos(3\varphi_r) + B\sin(3\varphi_r)$$

where:

$$\begin{cases} A = -\frac{3}{8}2\pi A_r^3 A_k \sin(\varphi_k) \\ B = \frac{3}{8}2\pi A_r^3 A_k \cos(\varphi_k) \end{cases} \tag{A7}$$

Third Term

$$\int_0^{2\pi} 3A_r s_r \left(\sum_{\substack{k=1 \\ k \neq r}}^{M} A_k \ s_k \right)^2 A_r c_r \, dt$$

$$= 3A_r^2 \int_0^{2\pi} s_r c_r \left(\sum_{\substack{k=1 \\ k \neq r}}^{M} A_k^2 s_k^2 + 2 \sum_{\substack{k,m \neq r \\ k > m}}^{M} A_k A_m s_k s_m \right) dt \tag{A8}$$

$$= \frac{3}{2}A_r^2 \sum_{\substack{k=1 \\ k \neq r}}^{M} A_k^2 \int_0^{2\pi} s_k^2 s_{2r} \, dt + 3A_r^2 \sum_{\substack{k,m \neq r \\ k > m}}^{M} A_k A_m \int_0^{2\pi} s_{2r} s_k s_m \, dt$$

Let us now analyze the two integrals in (A8) separately. For what concerns the first integral:

$$\frac{3}{2}A_r^2 \sum_{\substack{k=1 \\ k \neq r}}^{M} A_k^2 \int_0^{2\pi} s_k^2 \ s_{2r} \ dt = \frac{3}{2}A_r^2 \sum_{\substack{k=1 \\ k \neq r}}^{M} A_k^2 \int_0^{2\pi} (1 - c_{2k}) s_{2r} \ dt$$

$$= \frac{3}{2}A_r^2 \sum_{\substack{k=1 \\ k \neq r}}^{M} A_k^2 \int_0^{2\pi} s_{2r} \ dt - \frac{3}{2}A_r^2 \sum_{\substack{k=1 \\ k \neq r}}^{M} A_k^2 \int_0^{2\pi} s_{2r} c_{2k} \ dt = 0, \ \forall r$$

(A9)

The first integral in (A9) is null $\forall r$ because it is the integral of a sinusoid within a multiple of its period. The second integral leads to the sum of integrals whose argument is the product of two sinusoids with different frequency (because $k \neq r$); therefore, it is null $\forall r$.

Considering the second integral in (A8):

$$3A_r^2 \sum_{\substack{k,m \neq r \\ k > m}}^{M} A_k A_m \int_0^{2\pi} s_k s_m s_{2r} \ dt = \frac{3}{2}A_r^2 \sum_{\substack{k,m \neq r \\ k > m}}^{M} A_k A_m \int_0^{2\pi} (c_{k-m} - c_{k+m}) \ s_{2r} \ dt$$

$$= \frac{3}{2}A_r^2 \sum_{\substack{k,m \neq r \\ k > m}}^{M} A_k A_m \int_0^{2\pi} (s_{2r} c_{k-m} - s_{2r} c_{k+m}) \ dt \neq 0$$

$$\forall \, k,m : k \pm m = 2r$$

(A10)

Then, the integral in (A10) is not null for two cases, i.e., $k \pm m = 2r$.

$$\mp \tfrac{3}{2} A_r^2 \sum_{\substack{k \pm m = 2r \\ k,m \neq r \\ k > m}}^{M} A_k \quad A_m \int_0^{2\pi} s_{2r} c_{k \pm m} \ dt =$$

$$\mp \tfrac{3}{2} A_r^2 \sum_{\substack{k \pm m = 2r \\ k,m \neq r \\ k > m}}^{M} A_k A_m \int_0^{2\pi} sin(2rt + \varphi_r) cos((k \pm m)t + \varphi_k$$

$$\pm \varphi_m) \ dt =$$

$$\mp \tfrac{3}{4} A_r^2 \sum_{\substack{k \pm m = 2r \\ k,m \neq r \\ k > m}}^{M} A_k A_m \int_0^{2\pi} [sin((4rt + 2\varphi_r + \varphi_k \pm \varphi_m)$$

$$+ sin(2\varphi_r - \varphi_k \mp \varphi_m)] \ dt =$$

$$\pm \tfrac{3}{4} 2\pi A_r^2 \sum_{\substack{k \pm m = 2r \\ k,m \neq r \\ k > m}}^{M} A_k A_m sin(\varphi_k \pm \varphi_m - 2\varphi_r)$$

$$= \pm \tfrac{3}{4} 2\pi A_r^2 \sum_{\substack{k \pm m = 2r \\ k,m \neq r \\ k > m}}^{M} A_k A_m [sin(\varphi_k \pm \varphi_m) cos(2\varphi_r)$$

$$- cos(\varphi_k \pm \varphi_m) sin(2\varphi_r)] =$$

$$= \left[\pm \tfrac{3}{4} 2\pi A_r^2 \sum_{\substack{k \pm m = 2r \\ k,m \neq r \\ k > m}}^{M} A_k A_m sin(\varphi_k \pm \varphi_m) \right] cos(2\varphi_r)$$

$$+ \left[\mp \tfrac{3}{4} 2\pi A_r^2 \sum_{\substack{k \pm m = 2r \\ k,m \neq r \\ k > m}}^{M} A_k A_m cos(\varphi_k \pm \varphi_m) \right] sin(2\varphi_r)$$

$$= C cos(2\varphi_r) + D sin(2\varphi_r)$$

(A11)

where

$$\begin{cases} C = \pm \tfrac{3}{4} 2\pi A_r^2 \sum_{\substack{k \pm m = 2r \\ k,m \neq r \\ k > m}}^{M} A_k A_m \sin(\varphi_k \pm \varphi_m) \\ \\ D = \mp \tfrac{3}{4} 2\pi A_r^2 \sum_{\substack{k \pm m = 2r \\ k,m \neq r \\ k > m}}^{M} A_k A_m \cos(\varphi_k \pm \varphi_m) \end{cases}$$

(A12)

Fourth Term

$$\int\limits_0^{2\pi} \left(\sum_{\substack{k=1 \\ k \neq r}}^{M} A_k s_k \right)^3 A_r c_r \, dt = \int\limits_0^{2\pi} \left[\sum_{\substack{k=1 \\ k \neq r}}^{M} A_k^3 s_k^3 + 3 \sum_{\substack{k,l \neq r \\ k > l}}^{M} A_k A_l^2 s_k s_l^2 + 6 \sum_{\substack{k,l,m \neq r \\ k > l > m}}^{M} A_k A_l A_m s_k s_l s_m \right] A_r c_r \, dt \quad \text{(A13)}$$

Let us now analyze each term one by one.

1. Calculation of the term: $\int_0^{2\pi} \sum_{\substack{k=1 \\ k \neq r}}^{M} A_k^3 s_k^3 A_r c_r \, dt$

$$\int\limits_0^{2\pi} \sum_{\substack{k=1 \\ k \neq r}}^{M} A_k^3 s_k^3 A_r c_r \, dt = A_r \sum_{\substack{k=1 \\ k \neq r}}^{M} A_k^3 \int\limits_0^{2\pi} s_k^2 s_k c_r \, dt = \frac{A_r}{2} \sum_{\substack{k=1 \\ k \neq r}}^{M} A_k^3 \int\limits_0^{2\pi} (1 - c_{2k}) s_k c_r \, dt$$

$$= \frac{A_r}{2} \sum_{\substack{k=1 \\ k \neq r}}^{M} A_k^3 \int\limits_0^{2\pi} (s_k c_r - s_k c_{2k} c_r) \, dt \quad \text{(A14)}$$

The first addend in (A14) is null $\forall r$ because it leads to the sum of integrals whose argument is the product of two sinusoids with different frequency (because $k \neq r$).

Concerning the second addend:

$$-\frac{A_r}{2} \sum_{\substack{k=1 \\ k \neq r}}^{M} A_k^3 \int\limits_0^{2\pi} s_k c_{2k} c_r \, dt = -\frac{A_r}{4} \sum_{\substack{k=1 \\ k \neq r}}^{M} A_k^3 \int\limits_0^{2\pi} (s_{3k} - s_k) c_r \, dt$$

$$= -\frac{A_r}{4} \sum_{\substack{k=1 \\ k \neq r}}^{M} A_k^3 \int\limits_0^{2\pi} (s_{3k} c_r - s_k c_r) \, dt \quad \text{(A15)}$$

The second integral in (A15) is null $\forall r$ because it leads to the sum of integrals whose argument is the product of two sinusoids with different frequency (because $k \neq r$). Then, only the first addend survives leading to:

$$-\frac{A_r}{4} \sum_{\substack{k=1 \\ k \neq r}}^{M} A_k^3 \int\limits_0^{2\pi} s_{3k} c_r \, dt \neq 0 \ \forall \, k : k = \frac{r}{3} \quad \text{(A16)}$$

Then, the integral in (A16) is not null only for $k = \frac{r}{3}$:

$$-\frac{A_r}{4} \sum_{\substack{k=1 \\ k \neq r}}^{M} A_k^3 \int_0^{2\pi} \sin \quad (3kt + 3\varphi_k) \cos (rt + \varphi_r) dt$$

$$= -\frac{A_r}{8} \sum_{\substack{k=1 \\ k \neq r}}^{M} A_k^3 \int_0^{2\pi} [\sin(2rt + 3\varphi_k + \varphi_r) + \sin(3\varphi_k - \varphi_r)] dt$$

$$= -\frac{2\pi A_r A_k^3}{8} \sin(3\varphi_k - \varphi_r)$$

$$= \left[-\frac{2\pi A_r A_k^3}{8} \sin(3\varphi_k) \right] \cos(\varphi_r)$$

$$+ \left[\frac{2\pi A_r A_k^3}{8} \cos(3\varphi_k) \right] \sin(\varphi_r) = E \cos(\varphi_r) + F \sin(\varphi_r)$$

(A17)

where

$$\begin{cases} E = -\frac{2\pi A_r A_k^3}{8} \sin(3\varphi_k) \\ F = \frac{2\pi A_r A_k^3}{8} \cos(3\varphi_k) \end{cases}$$

(A18)

2. Calculation of the term: $\int_0^{2\pi} 3 \sum_{\substack{k,l \neq r \\ k > l}}^{M} A_k A_l^2 s_k s_l^2 A_r c_r \, dt$

$$\int_0^{2\pi} 3 \sum_{\substack{k,l \neq r \\ k > l}}^{M} A_k A_l^2 s_k \quad s_l^2 A_r c_r \, dt = 3A_r \sum_{\substack{k,l \neq r \\ k > l}}^{M} A_k A_l^2 \int_0^{2\pi} s_k s_l^2 \, c_r \, dt$$

$$= \frac{3}{2} A_r \sum_{\substack{k,l \neq r \\ k > l}}^{M} A_k A_l^2 \int_0^{2\pi} (1 - c_{2l}) s_k \, c_r \, dt$$

$$= \frac{3}{2} A_r \sum_{\substack{k,l \neq r \\ k > l}}^{M} A_k A_l^2 \int_0^{2\pi} (s_k c_r - s_k c_{2l} c_r) \, dt$$

(A19)

$$= -\frac{3}{2} A_r \sum_{\substack{k,l \neq r \\ k > l}}^{M} A_k A_l^2 \int_0^{2\pi} s_k c_{2l} c_r \, dt$$

$$= -\frac{3}{4} A_r \sum_{\substack{k,l \neq r \\ k > l}}^{M} A_k A_l^2 \int_0^{2\pi} (s_{k+2l} c_r + s_{k-2l} c_r) \, dt \neq 0$$

$$\forall k,l : k \pm 2l = r \, ; k > l$$

The integral (A19) is not null for two cases, i.e., $k \pm 2l = r$:

$$-\tfrac{3}{4}A_r \sum_{\substack{k \pm 2l = r \\ k,l \neq r}}^{M} A_k \; A_l^2 \int_0^{2\pi} s_{k\pm2l} c_r \, dt$$

$$= -\tfrac{3}{8}A_r \sum_{\substack{k \pm 2l = r \\ k,l \neq r}}^{M} A_k A_l^2 \int_0^{2\pi} [\sin(2rt + \varphi_k \pm 2\varphi_l + \varphi_r)$$

$$+ \sin(\varphi_k \pm 2\varphi_l - \varphi_r)] \, dt$$

$$= -\tfrac{3}{8}2\pi A_r \sum_{\substack{k \pm 2l = r \\ k,l \neq r \\ k > l}}^{M} A_k A_l^2 \sin(\varphi_k \pm 2\varphi_l - \varphi_r)$$

$$= \left[-\tfrac{3}{8}2\pi A_r \sum_{\substack{k \pm 2l = r \\ k,l \neq r \\ k > l}}^{M} A_k A_l^2 \sin(\varphi_k \pm 2\varphi_l) \right] \cos(\varphi_r) \tag{A20}$$

$$+ \left[\tfrac{3}{8}2\pi A_r \sum_{\substack{k \pm 2l = r \\ k,l \neq r \\ k > l}}^{M} A_k A_l^2 \cos(\varphi_k \pm 2\varphi_l) \right] \sin(\varphi_r)$$

$$= E \cos(\varphi_r) + F \sin(\varphi_r)$$

where:

$$\begin{cases} E = -\tfrac{3}{8}2\pi A_r \sum_{\substack{k \pm 2l = r \\ k,l \neq r \\ k > l}}^{M} A_k A_l^2 \sin(\varphi_k \pm 2\varphi_l) \\[2em] F = \tfrac{3}{8}2\pi A_r \sum_{\substack{k \pm 2l = r \\ k,l \neq r \\ k > l}}^{M} A_k A_l^2 \cos(\varphi_k \pm 2\varphi_l) \end{cases} \tag{A21}$$

3. Calculation of the term: $\int_0^{2\pi} 6 \sum_{\substack{k,l,m \neq r \\ k > l > m}}^{M} A_k A_l A_m s_k s_l s_m A_r c_r \, dt$

$$\int_0^{2\pi} 6 \sum_{\substack{k,l,m \neq r \\ k > l > m}}^{M} A_k A_l \quad A_m s_k s_l s_m \, dt = 6A_r \sum_{\substack{k,l,m \neq r \\ k > l > m}}^{M} A_k A_l A_m \int_0^{2\pi} s_k s_l s_m c_r \, dt$$

$$= 3A_r \sum_{\substack{k,l,m \neq r \\ k > l > m}}^{M} A_k A_l A_m \int_0^{2\pi} s_k (c_{l-m} - c_{l+m}) c_r \, dt$$

$$= \pm 3A_r \sum_{\substack{k,l,m \neq r \\ k > l > m}}^{M} A_k A_l A_m \int_0^{2\pi} s_k c_{l \mp m} c_r \, dt \tag{A22}$$

$$= \pm \frac{3}{2} A_r \sum_{\substack{k,l,m \neq r \\ k > l > m}}^{M} A_k A_l A_m \int_0^{2\pi} (s_{k+l \mp m} + s_{k-l \pm m}) c_r \, dt \neq 0$$

$$\forall \, k, l, m : k + l \mp m = r; \; k - l \pm m = r; k > l > m$$

The integral (A22) is not null in four cases, i.e., $k + l \mp m = r$; $k - l \pm m = r$. In particular, for: $k + l \mp m = r$

$$\pm \frac{3}{2} A_r \sum_{\substack{k+l \mp m \\ k,l,m \neq r \\ k > l > m}}^{M} A_k A_l \quad A_m \int_0^{2\pi} s_{k+l \mp m} c_r \, dt$$

$$= \pm \frac{3}{4} A_r \sum_{\substack{k+l \mp m \\ k,l,m \neq r \\ k > l > m}}^{M} A_k A_l A_m \int_0^{2\pi} [\sin(2rt + \varphi_k + \varphi_l \mp \varphi_m + \varphi_r)$$

$$+ \sin(\varphi_k + \varphi_l \mp \varphi_m - \varphi_r)] \, dt$$

$$= \pm \frac{3}{4} 2\pi A_r \sum_{\substack{k+l \mp m \\ k,l,m \neq r \\ k > l > m}}^{M} A_k A_l A_m \sin(\varphi_k + \varphi_l \mp \varphi_m - \varphi_r) \tag{A23}$$

$$= \left[\pm \frac{3}{4} 2\pi A_r \sum_{\substack{k+l \mp m \\ k,l,m \neq r}}^{M} A_k A_l A_m \sin(\varphi_k + \varphi_l \mp \varphi_m) \right] \cos(\varphi_r)$$

$$+ \left[\mp \frac{3}{4} 2\pi A_r \sum_{\substack{k+l \mp m \\ k,l,m \neq r}}^{M} A_k A_l A_m \cos(\varphi_k + \varphi_l \mp \varphi_m) \right] \sin(\varphi_r) =$$

$$= E \cos(\varphi_r) + F \sin(\varphi_r)$$

where

$$
\begin{cases}
E = \pm\frac{3}{4}2\pi A_r \sum\limits_{\substack{k+l\mp m \\ k,l,m \neq r \\ k>l>m}}^{M} A_k A_l A_m \sin(\varphi_k + \varphi_l \mp \varphi_m) \\
F = \mp\frac{3}{4}2\pi A_r \sum\limits_{\substack{k+l\mp m \\ k,l,m \neq r \\ k>l>m}}^{M} A_k A_l A_m \cos(\varphi_k + \varphi_l \mp \varphi_m)
\end{cases}
\tag{A24}
$$

The same exact procedure holds for the second case: i.e., for $k - l \pm m = r$

$$
\pm\frac{3}{2}A_r \sum\limits_{\substack{k-l\pm m \\ k,l,m \neq r \\ k>l>m}}^{M} A_k A_l \quad A_m \int\limits_{0}^{2\pi} s_{k-l\pm m} c_r \, dt
$$

$$
= \pm\frac{3}{4}A_r \sum\limits_{\substack{k+l\mp m \\ k,l,m \neq r}}^{M} A_k A_l A_m \int\limits_{0}^{2\pi} [\sin(2rt + \varphi_k - \varphi_l \pm \varphi_m + \varphi_r)
$$
$$
+ \sin(\varphi_k - \varphi_l \pm \varphi_m - \varphi_r)] \, dt
$$

$$
= \left[\pm\frac{3}{4}2\pi A_r \sum\limits_{\substack{k+l\mp m \\ k,l,m \neq r \\ k>l>m}}^{M} A_k A_l A_m \sin(\varphi_k - \varphi_l \pm \varphi_m) \right] \cos(\varphi_r)
$$

$$
+ \left[\mp\frac{3}{4}2\pi A_r \sum\limits_{\substack{k+l\mp m \\ k,l,m \neq r \\ k>l>m}}^{M} A_k A_l A_m \cos(\varphi_k - \varphi_l \pm \varphi_m) \right] \sin(\varphi_r) =
$$
$$
= E\cos(\varphi_r) + F\sin(\varphi_r)
\tag{A25}
$$

where

$$
\begin{cases}
E = \pm\frac{3}{4}2\pi A_r \sum\limits_{\substack{k+l\mp m \\ k,l,m \neq r \\ k>l>m}}^{M} A_k A_l A_m \sin(\varphi_k - \varphi_l \pm \varphi_m) \\
F = \mp\frac{3}{4}2\pi A_r \sum\limits_{\substack{k+l\mp m \\ k,l,m \neq r \\ k>l>m}}^{M} A_k A_l A_m \cos(\varphi_k - \varphi_l \pm \varphi_m)
\end{cases}
\tag{A26}
$$

Summarizing the previous results, for $k \pm (l \mp m) = r$

$$
\int\limits_{0}^{2\pi} 6 \sum\limits_{\substack{k,l,m \neq r \\ k>l>m}}^{M} A_k A_l A_m s_k s_l s_m \, dt = E\cos(\varphi_r) + F\sin(\varphi_r)
\tag{A27}
$$

where

$$
\begin{cases}
E = \pm\frac{3}{4}2\pi A_r \displaystyle\sum_{\substack{k+l\mp m \\ k,l,m \neq r \\ k>l>m}}^{M} A_k A_l A_m \sin[\varphi_k \pm (\varphi_l \mp \varphi_m)] \\
F = \mp\frac{3}{4}2\pi A_r \displaystyle\sum_{\substack{k+l\mp m \\ k,l,m \neq r \\ k>l>m}}^{M} A_k A_l A_m \cos[\varphi_k \pm (\varphi_l \mp \varphi_m)]
\end{cases}
\tag{A28}
$$

References

1. Jiang, T.; Xiang, W.; Chen, H.H.; Ni, Q. Multicast broadcasting services support in OFDMA-based WiMAX systems. *IEEE Comm. Mag.* **2007**, *45*, 78–86. [CrossRef]
2. Wu, Y.; Zou, W.Y. Orthogonal frequency division multiplexing: A multi-carrier modulation scheme. *IEEE Trans. Consum. Electron.* **1995**, *41*, 392–399.
3. Zou, W.Y.; Wu, Y. COFDM: An overview. *IEEE Trans. Broadcasting* **1995**, *41*, 1–8. [CrossRef]
4. Jiang, T.; Wu, Y. An Overview: Peak-to-Average Power Ratio Reduction Techniques for OFDM Signals. *IEEE Trans. Broadcasting* **2008**, *54*, 257–268. [CrossRef]
5. Galli, S.; Scaglione, A.; Dostert, K. Broadband Is Power: Internet Access Through the Power Line Network (Guest Editorial). *IEEE Commun. Mag.* **2003**, *41*, 82–83. [CrossRef]
6. Galli, S.; Scaglione, A.; Wang, Z. For the Grid and Through the Grid: The Role of Power Line Communications in the Smart Grid. *Proc. IEEE* **2011**, *99*, 998–1027. [CrossRef]
7. Fuller, J.F.; Fuchs, E.F.; Roesler, K.J. Review of Smart Grid Comprehensive Assessment Systems. *Energy Procedia* **2011**, *12*, 219–229.
8. Kolhe, M. Smart Grid: Charting a New Energy Future: Research, Development and Demonstration. *Electr. J.* **2012**, *25*, 88–93. [CrossRef]
9. *1901-2010*; Standard for Broadband over Power Line Networks: Medium Access Control and Physical Layer Specifications. IEEE: Piscataway, NJ, USA, 2010.
10. Han, S.H.; Lee, J.H. An overview of peak-to-average power ratio reduction techniques for multicarrier transmission. *IEEE Wirel. Commun.* **2005**, *12*, 56–65. [CrossRef]
11. Vijayarangan, V.; Sukanesh, R. An overview of techniques for reducing peak to average power ratio and its selection criteria for orthogonal frequency division multiplexing radio systems. *J. Theor. Appl. Inf. Technol.* **2009**, *5*, 25–36.
12. Rahmatallah, Y.; Mohan, S. Peak-to-average power ratio reduction in OFDM systems: A survey and taxonomy. *IEEE Commun. Surv. Tuts.* **2013**, *15*, 1567–1592. [CrossRef]
13. Sandoval, F.; Poitau, G.; Gagnon, F. Hybrid Peak-to-Average Power Ratio Reduction Techniques: Review and Performance Comparison. *IEEE Access* **2017**, *5*, 27145–27161. [CrossRef]
14. Jiang, T.; Zhu, G.X. Complement block coding for reduction in peak-to-average power ratio of OFDM signals. *IEEE Commun. Mag.* **2005**, *43*, S17–S22. [CrossRef]
15. Jones, A.E.; Wilkinson, T.A.; Barton, S.K. Block coding scheme for reduction of peak to mean envelope power ratio of multicarrier transmission schemes. *Electron. Lett.* **1994**, *30*, 2098–2099. [CrossRef]
16. Abouda, A.A. PAPR reduction of OFDM signal using turbo coding and selective mapping. In Proceedings of the 6th Nordic Signal Processing Symposium (NORSIG), Espoo, Finland, 9–11 June 2004; pp. 248–251.
17. Tsai, Y.C.; Deng, S.K.; Chen, K.C.; Lin, M.C. Turbo coded OFDM for reducing PAPR and error rates. *IEEE Trans. Wirel. Commun.* **2008**, *7*, 84–89. [CrossRef]
18. Qu, D.; Li, L.; Jiang, T. Invertible subset LDPC code for PAPR reduction in OFDM systems with low complexity. *IEEE Trans. Wirel. Commun.* **2014**, *13*, 2204–2213. [CrossRef]
19. Shu, S.; Qu, D.; Li, L.; Jiang, T. Invertible subset QC-LDPC codes for PAPR reduction of OFDM signals. *IEEE Trans. Broadcasting* **2015**, *61*, 290–298. [CrossRef]
20. Gokceli, S.; Kurt, G.K. Superposition coded-orthogonal frequency division multiplexing. *IEEE Access* **2018**, *6*, 14842–14856. [CrossRef]
21. Ren, G.L.; Zhang, H.; Chang, Y.L. A complementary clipping transform technique for the reduction of peak-to-average power ratio of OFDM system. *IEEE Trans. Consum. Electron.* **2003**, *49*, 922–926.
22. O'Neill, R.; Lopes, L.B. Envelope variations and spectral splatter in clipped multicarrier signals. In Proceedings of the 6th International Symposium on Personal, Indoor and Mobile Radio Communications, Toronto, ON, Canada, 27–29 September 1995; Volume 1, pp. 71–75.
23. Al-Jawhar, Y.A.; Ramli, K.N.; Mustapha, A.; Mostafa, S.A.; Shah, N.S.M.; Taher, M.A. Reducing PAPR with low complexity for 4G and 5G waveform designs. *IEEE Access* **2019**, *7*, 97673–97688. [CrossRef]

24. Bäuml, R.W.; Fischer, R.F.H.; Huber, J.B. Reducing the peak to average power ratio of multicarrier modulation by selected mapping. *Electron. Lett.* **1996**, *32*, 2056–2057. [CrossRef]

25. Lee, G.R.; Cheng, C.H.; Hung, H.L. Selected mapping applied scheme for PAPR reduction in OFDM communication systems. In Proceedings of the 6th International Conference on Networked Computing and Advanced Information Management, NCM, Seoul, Korea, 16–18 August 2010; pp. 752–755.

26. Taher, M.A.; Singh, M.J.; Ismail, M.; Samad, S.A.; Islam, M.T.; Mahdi, H.F. Post-IFFT-modified selected mapping to reduce the PAPR of an OFDM system. *Circuits Syst. Signal Process.* **2015**, *34*, 535–555. [CrossRef]

27. Muller, S.H.; Huber, J.B. OFDM with reduced peak-to-average power ratio by optimum combination of partial transmit sequences. *IEE Electron. Lett.* **1997**, *33*, 36–69. [CrossRef]

28. Al-Jawhar, Y.A.; Ramli, K.N.; Taher, M.A.; Shah, N.S.M.; Audah, L.; Sami, M.; Abbas, T. New low-complexity segmentation scheme for the partial transmit sequence technique for reducing the high PAPR value in OFDM systems. *ETRI J.* **2018**, *40*, 699–713. [CrossRef]

29. Nikookar, H.; Lidsheim, K.S. Random phase updating algorithm for OFDM transmission with low PAPR. *IEEE Trans. Broadcasting* **2002**, *48*, 123–128. [CrossRef]

30. Yoo, S.S.; Yoon, S.; Kim, S.Y.; Song, I. A novel PAPR reduction scheme for OFDM systems: Selective mapping of partial tones (SMOPT). *IEEE Trans. Consum. Electron.* **2006**, *52*, 40–43.

31. Mobasher, A.; Khandani, A.K. Integer-based constellation shaping method for PAPR reduction in OFDM systems. *IEEE Trans. Commun.* **2006**, *54*, 119–127. [CrossRef]

32. Nahar, A.K.; Gitaffa, S.A.; Ezzaldean, M.M.; Khleaf, H.K. FPGA implementation of MC-CDMA wireless communication system based on SDR-a review. *Rev. Inf. Eng. Appl.* **2017**, *4*, 1–19. [CrossRef]

33. Shawqi, F.S.; Audah, L.; Hammoodi, A.T.; Hamdi, M.M.; Mohammed, A.H. A Review of PAPR Reduction Techniques for UFMC Waveform. In Proceedings of the 4th International Symposium on Multidisciplinary Studies and Innovative Technologies (ISMSIT), Istanbul, Turkey, 22–24 October 2020; pp. 1–6.

34. Hussein, M.A.; Nahar, A.K.; Ali, A.H. A new hybrid approach for reducing the high PAPR in OFDM and F-OFDM systems with low complexity. In Proceedings of the 2nd Al-Noor International Conference for Science and Technology (2NICST2020), Baghdad, Iraq, 28–30 August 2020; pp. 57–62.

35. Sharma, P.; Verma, S. Reducing PAPR of OFDM based wireless systems using companding with convolutional codes. *Int. J. Distrib. Parallel Syst.* **2011**, *2*, 99–105. [CrossRef]

36. Thota, S.; Kamatham, Y.; Paidimarry, C.S. Analysis of Hybrid PAPR Reduction Methods of OFDM Signal for HPA Models in Wireless Communications. *IEEE Access* **2020**, *8*, 22780–22791. [CrossRef]

37. Niwareeba, R.; Cox, M.A.; Cheng, L. Low complexity hybrid SLM for PAPR mitigation for ACO OFDM. *ICT Express* 2021; *in press*. [CrossRef]

38. Nahar, A.K.; Hussein, M.A. A hybrid of the selected mapping and partial transmit sequence approaches for reducing the high peak average to power ratio based on multi-carrier systems—Review. *Comput. Sci. Inf. Technol.* **2022**, *3*, 10–21.

39. Li, X.; Cimini, L.J. Effect of clipping and filtering on the performance of OFDM. *IEEE Commun. Lett.* **1998**, *2*, 131–133.

40. Camplani, M.; Cannas, B.; Carcangiu, S.; Fanni, A.; Montisci, A.; Usai, M. Tabu-search procedure for PAPR reduction in PLC channels. In Proceedings of the IEEE International Symposium on Industrial Electronics (ISIE), Bari, Italy, 4–7 July 2010; pp. 2979–2983.

41. Grippo, L.; Lampariello, F.; Lucidi, S. A Nonmonotone Line Search Technique for Newton's Method. *SIAM J. Numer. Anal.* **1986**, *23*, 707–716. [CrossRef]

42. Stewart, J. *Calculus: Early Transcendentals*, 7th ed.; Cengage Learning: Belmont, CA, USA, 2012; p. 493. ISBN 978-0-538-49790-9.

43. Cheng, X.; Liu, D.; Shi, W.; Zhao, Y.; Li, Y.; Kong, D. A Novel Conversion Vector-Based Low-Complexity SLM Scheme for PAPR Reduction in FBMC/OQAM Systems. *IEEE Trans. Broadcasting* **2020**, *66*, 656–666. [CrossRef]

44. Bulusu, S.K.C.; Shaiek, H.; Roviras, D.; Zayani, R. PAPR reduction for FBMC-OQAM systems using dispersive SLM technique. In Proceedings of the 2014 11th International Symposium on Wireless Communications Systems (ISWCS), Barcelona, Spain, 26–29 August 2014; pp. 568–572.